Visible-light phototransistors based on InGaZnO and silver nanoparticles

Jiin Yu, Seung Won Shin, Kwang-Ho Lee, Jin-Seong Park, and Seong Jun Kang

Citation: Journal of Vacuum Science & Technology B, Nanotechnology and Microelectronics: Materials, Processing, Measurement, and Phenomena **33**, 061211 (2015); doi: 10.1116/1.4936113
View online: http://dx.doi.org/10.1116/1.4936113
View Table of Contents: http://avs.scitation.org/toc/jvb/33/6
Published by the American Vacuum Society

Articles you may be interested in

Amorphous InGaZnO ultraviolet phototransistors with double-stack Ga_2O_3/SiO_2 dielectric
Applied Physics Letters **102**, 221104 (2013); 10.1063/1.4808164

High responsivity of amorphous indium gallium zinc oxide phototransistor with Ta_2O_5 gate dielectric
Applied Physics Letters **101**, 261112 (2012); 10.1063/1.4773307

Amorphous indium-gallium-zinc-oxide visible-light phototransistor with a polymeric light absorption layer
Applied Physics Letters **97**, 203506 (2010); 10.1063/1.3517506

Solution-processed PCDTBT capped low-voltage $InGaZnO_x$ thin film phototransistors for visible-light detection
Applied Physics Letters **106**, 242102 (2015); 10.1063/1.4922642

Photosensitivity of InZnO thin-film transistors using a solution process
Applied Physics Letters **109**, 132105 (2016); 10.1063/1.4963881

Anomalous high photoconductivity in short channel indium-zinc-oxide photo-transistors
Applied Physics Letters **106**, 013503 (2015); 10.1063/1.4905310

HIDEN ANALYTICAL
Instruments for Advanced Science

Gas Analysis
- dynamic measurement of reaction gas streams
- catalysis and thermal analysis
- molecular beam studies
- dissolved species probes
- fermentation, environmental and ecological studies

Surface Science
- UHV TPD
- SIMS
- end point detection in ion beam etch
- elemental imaging - surface mapping

Plasma Diagnostics
- plasma source characterization etch and deposition process reaction
- kinetic studies
- analysis of neutral and radical species

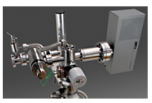
Vacuum Analysis
- partial pressure measurement and control of process gases
- reactive sputter process control
- vacuum diagnostics
- vacuum coating process monitoring

Contact Hiden Analytical for further details:
W www.HidenAnalytical.com
E info@hiden.co.uk
CLICK TO VIEW our product catalogue

Visible-light phototransistors based on InGaZnO and silver nanoparticles

Jiin Yu and Seung Won Shin
Department of Advanced Materials Engineering for Information and Electronics, Kyung Hee University, 1732 Deogyeong-daero, Giheung-gu, Yongin, Gyeonggi-do 446-701, Republic of Korea

Kwang-Ho Lee and Jin-Seong Park
Division of Materials Science and Engineering, Hanyang University, 222 Wangsimni-ro, Seoul 133-719, Republic of Korea

Seong Jun Kang[a)]
Department of Advanced Materials Engineering for Information and Electronics, Kyung Hee University, 1732 Deogyeong-daero, Giheung-gu, Yongin, Gyeonggi-do 446-701, Republic of Korea

(Received 22 July 2015; accepted 5 November 2015; published 23 November 2015)

Visible-light phototransistors were fabricated using wide-bandgap indium gallium zinc oxide (IGZO) and silver (Ag) nanoparticles (NPs). A bottom gate made of thin film transistors (TFTs) was fabricated with an amorphous IGZO film as the active channel. Ag NPs were then formed on the surface of the active channel region to be used as a visible-light absorption layer. The prepared Ag NPs were highly absorptive in the wavelength range of 450–600 nm, due to the plasmon effect. A detailed study of photoresponsivity and external quantum efficiency indicated that the TFTs with Ag NPs induced a large photocurrent upon illumination by visible light on the active region, while the TFTs without Ag NPs did not. This result indicates the presence of coupling between the localized plasmons and electrical carriers on the IGZO TFTs with Ag NPs. © *2015 American Vacuum Society*. [http://dx.doi.org/10.1116/1.4936113]

I. INTRODUCTION

Various investigators have used small-bandgap semiconducting materials such as silicon to try to develop a visible-light phototransistor.[1,2] Silicon has a bandgap of 1.1 eV, which is small enough to absorb a wide range of visible light,[3] and full-color image sensors have been successfully developed based on silicon.[4] Transparent electronics are a rapidly growing research field[5,6] and there have been many studies demonstrating the fabrication of transparent phototransistors.[7] Generally, a wide-bandgap indium gallium zinc oxide (IGZO) is chosen as the semiconducting material for transparent phototransistors.[8] However, the IGZO phototransistors cannot respond to visible light due to the wide bandgap of IGZO; they can only absorb high-energy photons, such as ultraviolet (UV) light. Thus, the application of IGZO phototransistors has been restricted to UV photosensors.[9] There is a need for a method of developing a transparent IGZO phototransistor that can respond to the low-energy photons such as those in visible and infrared light.

Several methods for improving the visible-light photoresponse of the IGZO phototransistors have been reported. These methods work by integrating a visible-light absorption layer into the IGZO device. Thin films of organic layers, quantum dots, and metal nanoparticles (NPs) have been used to improve the visible-light photoresponse.[10–12] Metal NPs improve the photocurrent due to the plasmon effect. Gold and silver (Ag) NPs induce a strong plasmon resonance with a wide range of visible light, which increases the photocurrent.[13,14] Therefore, integrating metal NPs on the device has been considered as a suitable approach to develop a visible-light photosensor using a wide-bandgap oxide semiconductor. In addition, a phototransistor based on oxide semiconductors and metal NPs has been demonstrated previously.[15] However, there have been few attempts to study the detailed photoresponses of IGZO phototransistors with metal NPs.

In this study, we fabricated a phototransistor using a wide-bandgap IGZO and Ag NPs to study the photoresponse of the plasmonic device in detail. The Ag NPs on the IGZO surface induced a strong plasmon resonance that increased the photocurrent. Various wavelengths of light illumination were applied to the device to study the photoresponsivity and external quantum efficiency (EQE) of the IGZO phototransistor with Ag NPs. In addition, the origin of the visible-light photocurrent was considered in detail.

II. EXPERIMENT

IGZO films of various thicknesses were deposited on SiO_2 (100 nm)/Si substrates by radio frequency sputtering. The composition ratio of the single target was In_2O_3:Ga_2O_3:ZnO = 1:1:1 at. %. Next, 100-nm long aluminum source and drain electrodes were fabricated on the surface of the IGZO film with a photolithography process and thermal evaporator. The channel length and width were 25 and 200 μm, respectively. Then, the buffered oxide etchant was used to isolate the active channel region of the device. For the plasmonic device, Ag NPs were synthesized on the surface of the IGZO using a thermal evaporator and postannealing process. A small amount of Ag was deposited onto the IGZO surface with an evaporation rate of 0.02 nm/s, which was monitored carefully using a calibrated quartz crystal microbalance. Then, a thin layer of Ag was annealed at 260 °C for 1 h with a flow of Ar gas.[15] The distribution of the Ag NPs and the channel region of the device were

[a)]Author to whom correspondence should be addressed; electronic mail: junkang@khu.ac.kr

 © 2015 American Vacuum Society

confirmed using scanning electron microscopy (SEM). The absorbances of the IGZO films with and without Ag NPs were measured using a UV/visible spectrometer. The electrical properties and photoresponse of the prepared device were characterized using a semiconductor parameter analyzer (HP 4145B) with various light sources. The wavelengths of the light sources were 405, 532, 635, and 780 nm.

III. RESULTS AND DISCUSSION

Thin film transistors (TFTs) using 10-nm-thick IGZO films were fabricated with an aluminum source and drain electrodes, as shown in Fig. 1. Then, the photoresponse of the device was characterized by measuring the transfer curves with and without illumination by high energy photons ($\lambda = 405$ nm) on the active channel region. An increase in current between the source and drain electrodes was observed with the illumination, as shown in Fig. 1. The applied drain voltage was 2 V during the measurement. The IGZO TFTs induced a photocurrent with the illumination, which had a higher energy than the bandgap of IGZO.

To examine the photoresponses in more detail, the responsivities and EQEs of the IGZO TFTs were characterized as a function of the thickness of the IGZO films and the illumination wavelengths of 405, 532, 635, and 780 nm. The responsivity of each device was evaluated by the equation

$$\text{Responsivity} = \frac{(I_{\text{total}} - I_{\text{dark}})/A_{pt}}{\text{P}/A_{pd}} = \frac{J_{ph}}{P}. \quad (1)$$

Here, I_{total} is the total current on the device, I_{dark} is the dark current, P is the incident power of the illumination, A_{pt} is the product of channel width and thickness, A_{pd} is the spot size of the laser source, J_{ph} is the photocurrent density, and P is the incident laser power density.[16] The EQE was calculated according to the following equation:

$$\text{EQE} = \frac{J_{ph}/q}{P/h\nu}. \quad (2)$$

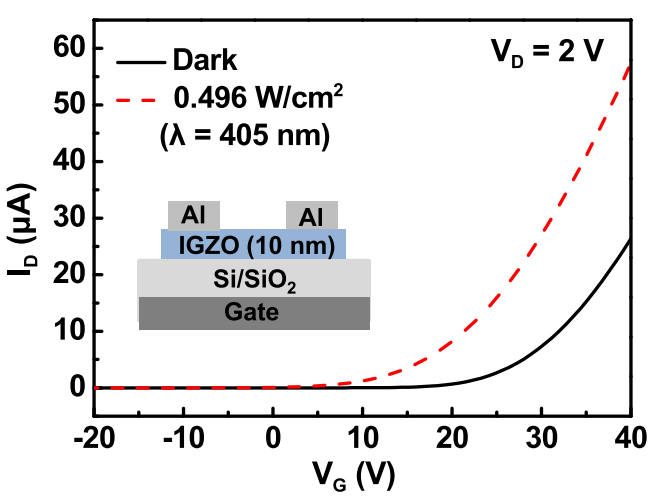

FIG. 1. (Color online) Transfer curves of the 10-nm IGZO TFT with and without illumination ($\lambda = 405$ nm). The inset shows the device structure.

Here, q is the charge and $h\nu$ is the photon energy.[16] The responsivities and EQEs of the TFTs with different thicknesses of IGZO films are shown in Fig. 2(a). Both the responsivities and the EQEs increased as the thicknesses of the IGZO films were reduced. Therefore, a thin layer of IGZO was sufficient to absorb the photons and induce a photocurrent. Figure 2(b) shows the responsivities and EQEs as a function of the illumination wavelength. The wide-bandgap IGZO films effectively induced a photocurrent with high-energy photons ($\lambda = 405$ nm). However, the responsivity and EQE were negligible when the photon energy was smaller than the bandgap of the IGZO film. Therefore, the IGZO TFTs could not induce a photocurrent with low-energy visible light due to the wide bandgap of the IGZO film.

To improve the photoresponse of the IGZO TFTs to low-energy visible light, Ag NPs were formed on the surfaces of IGZO films, as shown in Fig. 3(a). The inset of Fig. 3(a) shows the uniform distribution of Ag NPs at the channel region of the device. Figure 3(b) illustrates the UV/visible spectrometer measurements of IGZO (10 nm) and Ag NP/IGZO (10 nm) films on glass substrates. As shown in the figure, the absorbance of the 10-nm-thick IGZO film was almost negligible over a wide range of illumination wavelengths. However, enhanced absorbance was observed at the

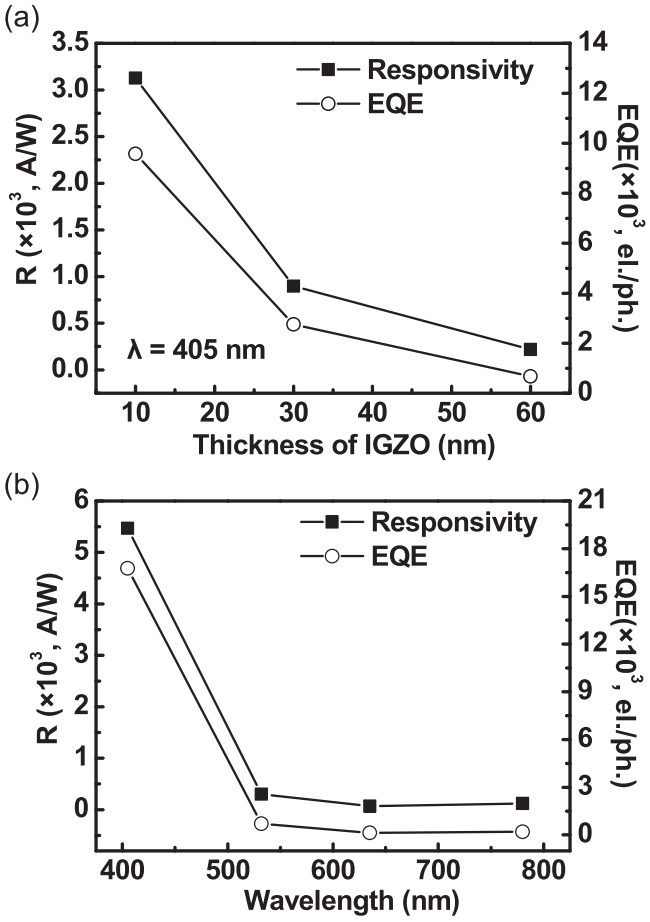

FIG. 2. (a) Responsivities and EQEs of the IGZO TFTs with various thicknesses of IGZO films. (b) The responsivities and EQEs of the IGZO TFTs as a function of the illumination wavelength.

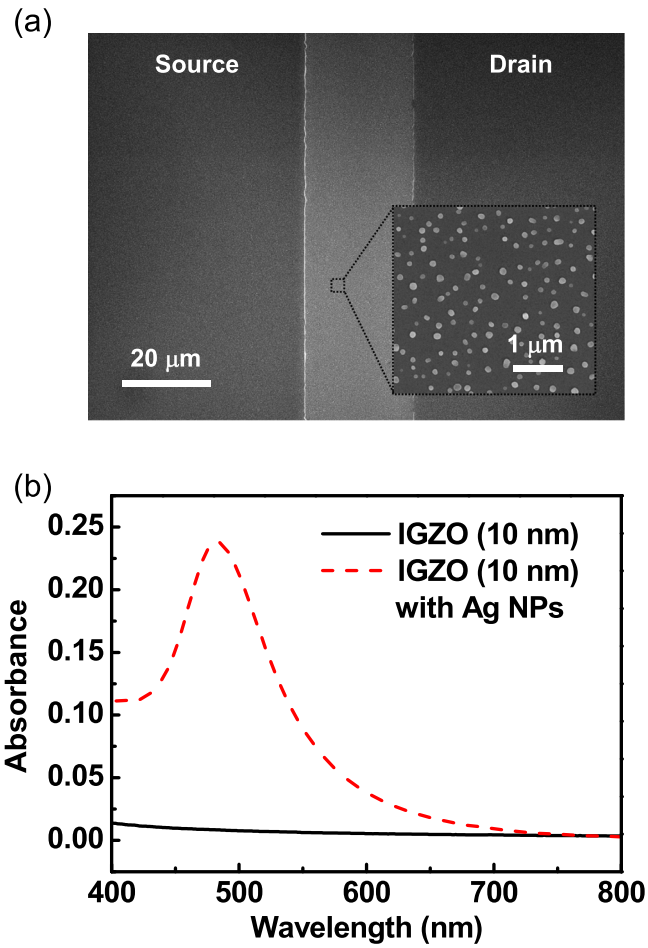

FIG. 3. (Color online) (a) SEM image of Ag NPs on the IGZO channel region. (b) UV/visible spectrometer measurements of 10-nm IGZO films with and without Ag NPs on their surfaces.

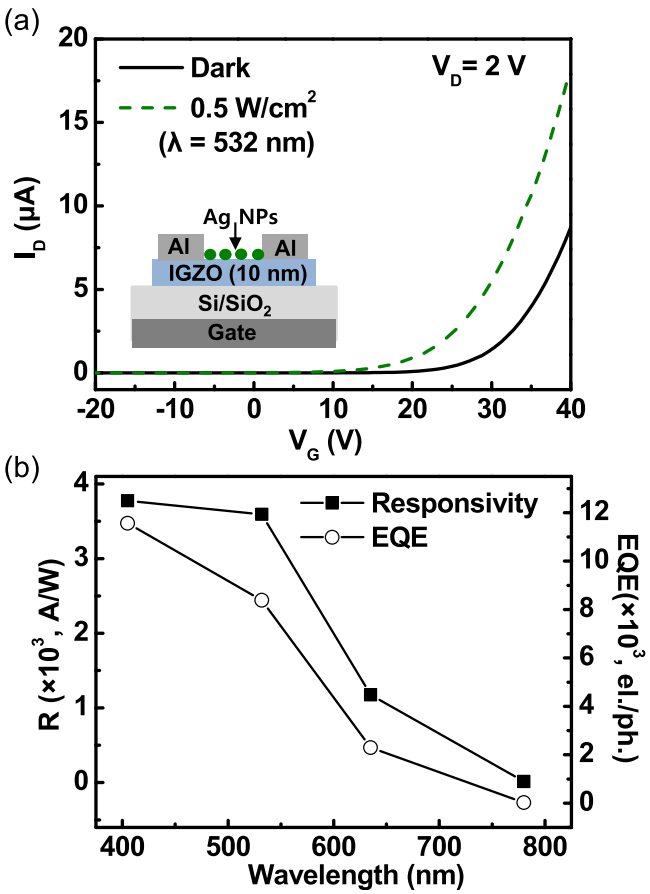

FIG. 4. (Color online) (a) Transfer curves of the plasmonic IGZO TFT with and without visible-light illumination ($\lambda = 532$ nm). The inset shows the device structure, where the Ag NPs are distributed on the IGZO surface. (b) The responsivities and EQEs of the plasmonic IGZO TFTs as a function of illumination wavelength.

wavelengths from 450 to 600 nm when the Ag NPs were positioned on the IGZO surfaces. This indicates a high level of plasmon absorption in the visible-light region with the Ag NPs. The peak position was 483 nm, which can be defined as the plasmon resonance wavelength attributed to the Ag NPs. Figure 4(a) shows the transfer curves of the IGZO TFTs, where the Ag NPs were coated on the surface of the IGZO. A laser source of 532 nm wavelength illuminated the channel region of the device during the measurements. An increase in photocurrent was observed with visible-light illumination due to the Ag NPs. The current between the drain and source electrodes was increased by 109% at $V_G = 40$ V. The dark current was not affected significantly by the Ag NPs. This implies that the plasmon resonance of Ag NPs can induce additional carriers in the channel region of the device. When responsivities and EQEs were evaluated as a function of illumination wavelength, the results further confirmed the plasmon effect was occurring in the device. As shown in Fig. 4(b), the responsivity and EQE were increased when the device was illuminated by 532-nm visible light, due to the Ag NPs. However, the responsivity and EQE were reduced with the 635-nm light source and were negligible with the 780-nm light source. The evaluated responsivities and EQEs in Fig. 4(b) were consistent with the absorbance spectrum in Fig. 3(b).

Figure 5 demonstrates the origin of the increased photocurrent between the drain and source electrodes of the IGZO TFTs patterned with Ag NPs. Generally, IGZO TFTs can only absorb high-energy photons, such as UV light, due to the intrinsically wide bandgap of IGZO. However, when the Ag NPs were distributed on the channel region, they induced a plasmon resonance with a low-energy visible light. The plasmon resonance of the Ag NPs induced additional carriers, which were injected into the conduction band of

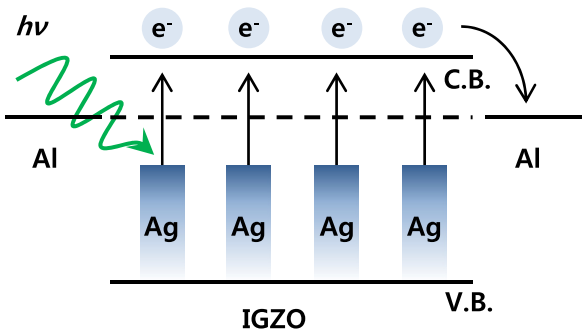

FIG. 5. (Color online) (a) Schematic of the mechanism of increased photocurrent due to the Ag NPs on the IGZO TFTs. C.B. is a conduction band, and V.B. is a valence band.

IGZO. Therefore, the Ag NPs improved the photoresponse of the wide-bandgap IGZO TFTs to low-energy visible light due to plasmon resonance.

IV. CONCLUSIONS

The plasmon effect was used to improve the visible-light photoresponse of wide-bandgap IGZO TFTs by patterning the IGZO channel region with Ag NPs. The absorbance measurements showed that plasmon resonance occurred over a wide range of visible light wavelengths due to the Ag NPs on the surface of the IGZO films. A significant increase in photocurrent in the Ag NP/IGZO TFTs was observed with the visible-light illumination. A detailed evaluation of responsivity and EQE indicated that plasmon resonance is the origin of the increase in photocurrent with visible-light illumination. Therefore, with more detailed studies of photoresponse time, these results will provide a useful method for improving the visible-light photoresponse of wide-bandgap oxide semiconductors for transparent visible-light phototransistor applications.

ACKNOWLEDGMENTS

This work was supported by the Center for Advanced Soft Electronics funded by the Ministry of Science, ICT and Future Planning as a Global Frontier Project (CASE-2014M3A6A5060946). It was also supported by a grant from the National Research Foundation of Korea (NRF-2013R1A1A1A05007934).

[1]Y. Kaneko, N. Koike, K. Tsutsui, and T. Tsukada, Appl. Phys. Lett. **56**, 650 (1990).
[2]K. Abid, A. Z. Khokhar, and F. Rahman, Sensor. Actuators A-Phys. **172**, 434 (2011).
[3]Z. Chen, T. Lee, and G. Bosman, Appl. Phys. Lett. **64**, 3446 (1994).
[4]D. Knipp, R. A. Street, H. Stiebig, M. Krause, J. P. Lu, S. Ready, and J. Ho, IEEE Trans. Electron Devices **53**, 1551 (2006).
[5]G. Lee *et al.*, ACS Nano **7**, 7931 (2013).
[6]J. Yoon *et al.*, Small **9**, 3295 (2013).
[7]H. S. Lee, S. Min, Y. Chang, M. K. Park, T. Nam, H. Kim, J. H. Kim, S. Ryu, and S. Im, Nano Lett. **12**, 3695 (2012).
[8]T. H. Chang, C. J. Chiu, W. Y. Weng, S. J. Chang, T. Y. Tsai, and Z. D. Huang, Appl. Phys. Lett. **101**, 261112 (2012).
[9]T. H. Chang, C. J. Chiu, S. J. Chang, T. Y. Tsai, T. H. Yang, Z. D. Huang, and W. Y. Weng, Appl. Phys. Lett. **102**, 221104 (2013).
[10]H. Zan, W. Chen, H. Hsueh, S. Kao, M. Ku, C. Tsai, and H. Meng, Appl. Phys. Lett. **97**, 203506 (2010).
[11]D. C. Oertel, M. G. Bawendi, A. C. Arango, and V. Bulović, Appl. Phys. Lett. **87**, 213505 (2005).
[12]D. M. Schaadt, B. Feng, and E. T. Yu, Appl. Phys. Lett. **86**, 063106 (2005).
[13]J. Miao *et al.*, Small **11**, 2392 (2015).
[14]R. Zakaria, W. K. Lin, and C. C. Lim, Appl. Phys. Express **5**, 082002 (2012).
[15]S. J. Park, S. M. Lee, S. J. Kang, K. Lee, and J. Park, J. Vac. Sci. Technol. A **33**, 021101 (2015).
[16]Y. Lee, I. Omkaram, J. Park, H. Kim, K. Kyung, W. Park, and S. Kim, IEEE Electron Device Lett. **36**, 41 (2015).